DATA MINE

TexNet: A Statewide Seismological Network in Texas

by Alexandros Savvaidis, Bissett Young, Guo-chin Dino Huang, and Anthony Lomax

ABSTRACT

Induced seismic events have been recorded recently in the southern midcontinent of the United States, including Texas. These events, associated with hydrocarbon exploration and the subsequent disposal of wastewater byproduct, have led to substantial public discussion regarding cause, public safety, and potential risks of damage to infrastructure. In an effort to better understand these events and to monitor earthquake activity in general, the 84th Texas Legislature funded creation of a statewide, seismic-monitoring program known as the Texas Seismological Network (TexNet). The goal of TexNet is to provide authenticated data to evaluate the location, frequency, and likely causes of natural and induced earthquakes, so TexNet, through August 2018, deployed 58 new broadband seismic stations in the state of Texas. Of these, 25 are permanent and form, along with 18 existing broadband stations, an evenly spaced backbone, seismic network in the state. In addition to the permanent installations, 33 of the new stations are portable and have been deployed in four different areas of the state experiencing recent seismicity and having high-socioeconomic importance. An earthquake-management system (SeisComp3) is being used to detect, locate, and analyze earthquake events and earthquakes measuring M_L 2 and above have been made available through various dissemination tools by the next working day. Depending on daily earthquake rate, events of magnitude down to 1.5 are publicly available in three business days from the time they are detected. The initial implementation of TexNet has reduced the magnitude of completeness (M_c) across Texas from 2.7 to less than 1.5 in specific areas and has played a role in a large decrease in uncertainties about earthquake-source parameters.

Supplemental Content: Tables listing the borehole stations site assessment and installation and the *P*- and *S*-wave velocities of the Earth model used for earthquake location in the Delaware basin are presented, and noise analysis of sites visited for deployment of a permanent station, classification of noise levels for Texas Seismological Network (TexNet) stations, a worldwide map where SeisComP3 (SCP3) installations in 2018, and a list of seismological observatories that SCP3 used.

INTRODUCTION

Because of the recent increase in seismicity in the southern midcontinent of the United States (Ellsworth, 2013; Weingarten *et al.*, 2015) and the history of earthquakes in Texas (Frohlich and Davis, 2002; Frohlich *et al.*, 2016), the state of Texas in 2015 funded the Texas Seismological Network (TexNet). The intent was to develop and install a seismological network throughout Texas; collect, analyze, and catalog data and make them publicly available at improved resolution; and conduct research leading to an understanding of the nature and causes of the seismicity (e.g., earthquakes).

A previously existing network of 18 operating seismic-monitoring stations, irregularly distributed across Texas, was not sufficient to detect, locate, and properly characterize seismicity at a level of accuracy necessary for an understanding either of what caused the event or whether any actions could be taken to reduce the recurrence of such events. Hence, the new TexNet seismic-monitoring network was created, which consists of stand-alone, broadband seismometers installed in suitable locations throughout Texas in two configurations—permanent and portable. As of August 2018, TexNet had installed 22 borehole and 3 auxiliary stations that, combined with the 18 previously existing stations, form a backbone seismic network of 43 stations, all of which enable the monitoring and cataloging of seismicity evenly across Texas. Interstation distance for the backbone network varies from 90 to 150 km. In addition to this backbone network, 33 portable seismic-monitoring stations were deployed to allow detailed site-specific assessments of areas of active seismicity. The portable stations were designed using broadband seismometers and accelerometers to allow onscale recording and detailed characterization of ground motion, even for large, nearby earthquakes.

TexNet uses an operational earthquake-management system (EMS) for detection, analysis, location, and dissemination of earthquake data, and quality-assurance information is obtained from a noise analysis of ground-motion data. In

doi: 10.1785/0220180350

addition, a comparison of earthquake-analysis information is presented from the existing stations, the new backbone stations, and the portable deployments. TexNet began providing earthquake data for Texas in January 2017. The purpose of this article is to introduce TexNet (code TX; see Data and Resources) and, more specifically, its design criteria, architecture, site evaluation, the quality assurance (QA) of stations, and an evaluation of seismicity characterization.

REQUISITE FOR TEXNET

Instrumental seismology for earthquakes in Texas began in 1970, when the first seismic station was deployed in the state. Earthquakes were recorded in Texas from 1973 through 2015, as reported in the U.S. Geological Survey Advanced National Seismic System (USGS/ANSS) Comprehensive Catalog (ComCat, see Data and Resources; Fig. 1). The earthquakes recorded during this period are all above the network magnitude of completeness (M_c) for the network, which is the minimum magnitude above which all earthquakes within a certain region are reliably recorded (Fig. 1). According to the ANSS catalog and the methods (goodness of fit [GFT], maximum curvature [MAXC]) of Mignan and Woessner (2012), the M_c for Texas for the period of 1973 through 2015 is 2.7. Mignan and Woessner (2012) used the frequency–magnitude distribution (FMD) of an earthquake catalog and calculated M_c through a GFT test (Wiemer and Wyss, 2000), as well as a MAXC technique (Wyss *et al.*, 1999; Wiemer and Wyss, 2000).

The rate of recorded seismicity has clearly been increasing in Texas (Fig. 1), beginning around 2008 (Frohlich and Davis, 2002; Frohlich *et al.*, 2016). Prior to that time, one to two earthquakes per year of $M \geq 3$ were recorded, on average. Since 2008, however, the rate has increased to approximately 15 events per year, on average. The frequency and cumulative number of earthquakes for the state of Texas are reported in the ANSS ComCat (see Data and Resources) and that from 1973 to 2015, the number of seismometers in Texas increased from 1 to 18. Also this increase in instruments in Texas does not influence the increase in recorded earthquakes above M 2.7 because we are presenting only events greater than the M_c for the period in question.

NETWORK

Design Criteria and Architecture of TexNet

A seismic network was designed using specific criteria on the basis of its intended purpose. The goals of TexNet are to (1) monitor, locate, and catalog seismicity across Texas and (2) facilitate the investigation of ongoing earthquake sequences by deploying portable seismic-monitoring stations. These site-specific assessments are most critical for events in or near urban areas or sites of large-scale human industrial and socioeconomic activities such as petroleum extraction, mining, and water infrastructure.

To support these goals, TexNet includes both permanent and portable stations. Permanent-station deployments have either a broadband (120 s) posthole seismometer for borehole (20 ft) installation or a broadband (20 s) posthole seismometer for direct-burial installation (3–5 ft). Portable-station deployments have a broadband (20 s) posthole seismometer (3–5 ft) and a $4g$ posthole accelerometer (1 ft) for direct-burial installation. TexNet permanent stations complement the existing broadband network in the state for an evenly grid-spaced backbone array. Portable stations are deployed closer to the earthquake source for better characterization of earthquake sequences, rupture zones, and local ground motion.

The following are considered primary criteria in the final selection of locations for new permanent stations: (1) locations of the 18 existing permanent Seismic Network stations in Texas, (2) locations of seismic stations in neighboring states, and (3) historical seismicity in Texas (as reported by ComCat; Fig. 2). At the end of 2017, Texas had 22 new borehole stations and 3 auxiliary, direct-burial stations (CRHG, HNVL, and DRIO) as part of the permanent array. The purpose of auxiliary stations, which use portable-station hardware although for an expectedly long-term plan of deployment, is to fill gaps in the backbone array. Together, existing and new stations are located over an approximately evenly spaced grid that provides optimal coverage across the entire state (Fig. 2). Specific locations were identified following a site-specific assessment for each of the 25 new permanent-station locations using a buffer zone with a radius of 25 mi. Numerous sites were evaluated within these buffer zones to determine optimal locations for station installations.

Considerations for portable-station deployment (Fig. 2) included recent seismicity (from 2013 onward), as well as the scientific and socioeconomic implications of the region. As of August 2018, TexNet had deployed 33 portable stations, distributed across the following general locations:

- 15 stations in the Fort Worth basin,
- 7 stations near Cogdell field,
- 8 stations in the Permian basin, and
- 3 stations in the Eagle Ford operating area.

Three portable stations are kept available for immediate deployment, depending on field conditions, to be complementary to existing TexNet deployments. The portable-station deployment plan is reevaluated yearly by TexNet.

Seismic Stations

Site Selection

Both permanent and portable station sites have roughly common criteria, including (1) station sites with low ambient noise and, where possible, (2) station sites with bedrock or an otherwise stiff substratum. Because of the different time spans of station deployment (6+ months for portable and 10 + yr for permanent) and different spacing (close spacing for portable and regional spacing for permanent), site-selection criteria and installation methods differ for the two types of deployment. Site assessment began on March 2016 and continued through July 2017.

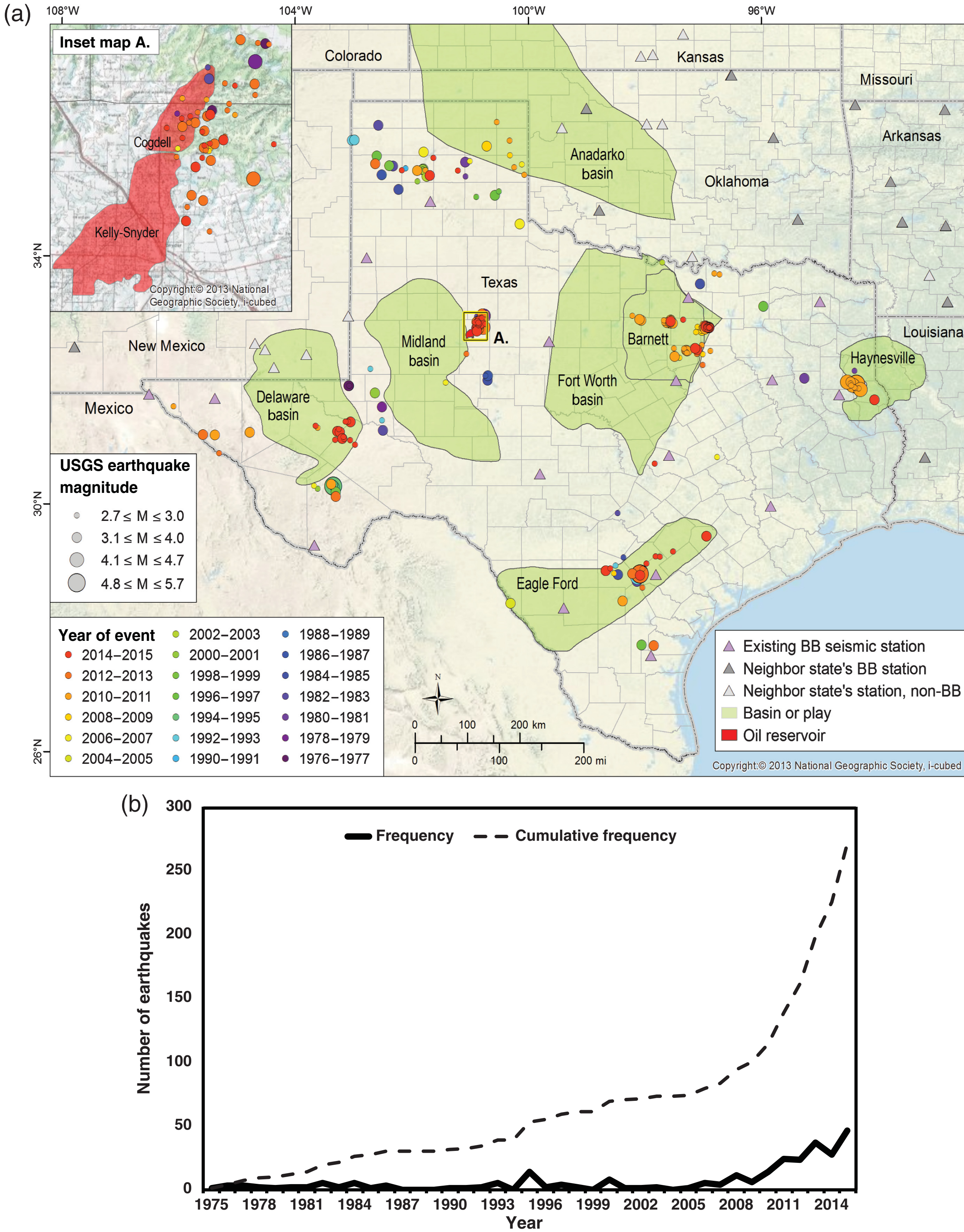

▲ **Figure 1.** (a) Map of Texas with seismicity of $M_L > 2.7$ from 1973 through 2015. Color coding follows time; only earthquakes larger than magnitude 2.7 are shown. Inset map A denotes the Kelly-Snyder and Cogdell oil fields. (b) Frequency (solid line) and cumulative number (dashed line) with time for earthquakes having $M \geq 2.7$. Data provided by U.S. Geological Survey Advanced National Seismic System (USGS/ANSS) catalog. BB, broadband.

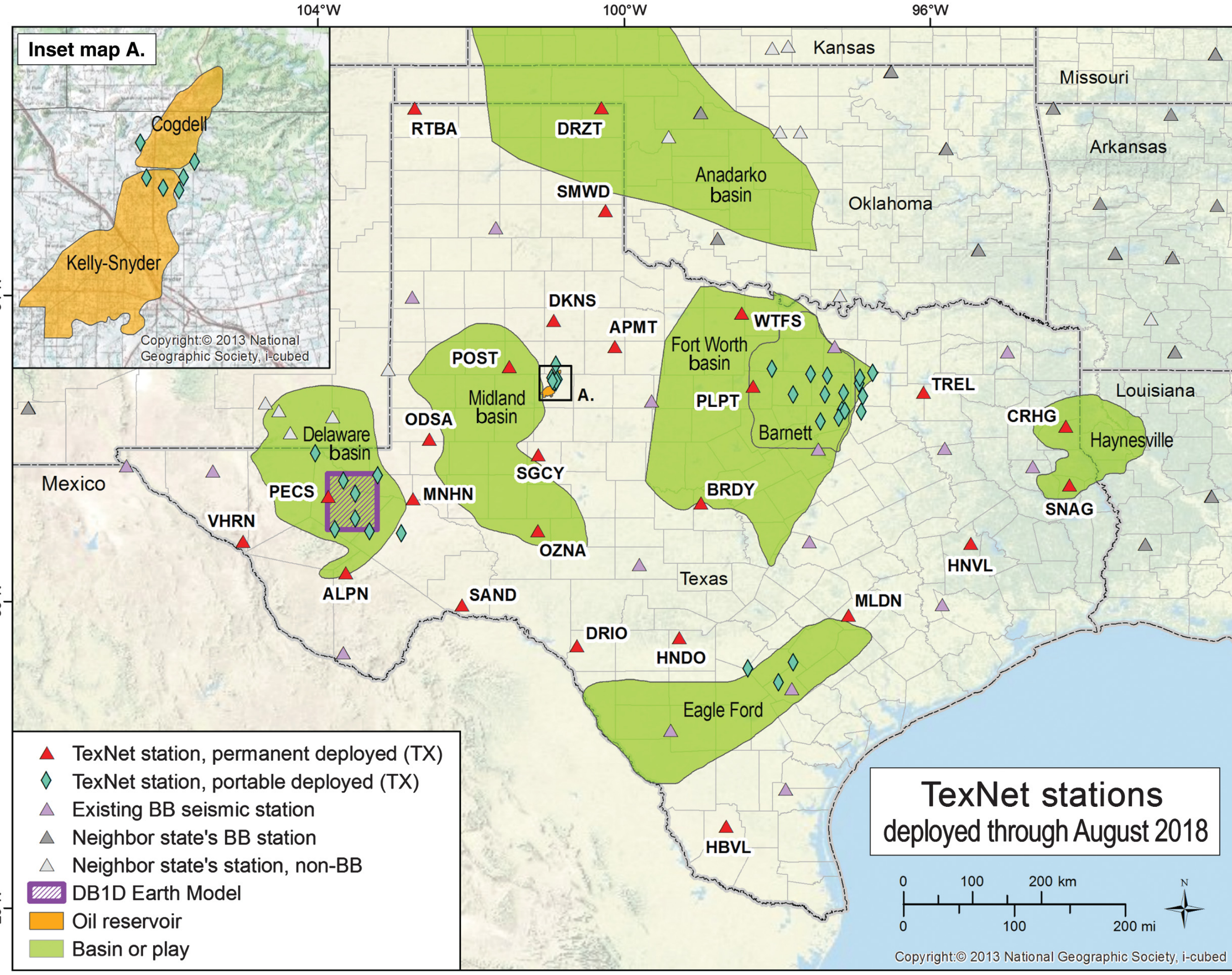

▲ **Figure 2.** Map of existing and newly deployed stations (TX International Federation of Digital Seismograph Networks [FDSN] network code). For Delaware basin area (magenta polygon), 1D Earth model (DB1D) calculated. Existing BB stations (magenta triangles) and newly deployed permanent stations (red triangles) are the backbone of Texas Seismological Network (TexNet) network. Inset map A denotes the Kelly-Snyder and Cogdell oil fields.

Permanent Sites. Permanent seismic-station installations include either placement of seismometers in 20-ft-deep cased and cemented boreholes (22 sites) or direct-burial in shallow (1–3 ft) pits (three sites). Of the 25 permanent stations, PECS and MNHN (Fig. 2) include deployment of an accelerometer. Once potential sites for permanent installations were identified, the corresponding landowners were contacted for access to the locations identified, and initial site assessment began. The agreement between TexNet (The University of Texas at Austin) and landowners uses a 10 yr license agreement for the sites ultimately selected for installation.

To facilitate site selection of the permanent stations (Fig. 2), performance of transportable array (TA) sites from EarthScope's USArray program, which was deployed in Texas from 2008 to 2011, was used to assess ambient noise and earthquake-monitoring effectiveness. Performance criteria included long-term noise as measured by station power spectral probability density function (McNamara *et al.*, 2009; Casey *et al.*, 2018), geologic description of the site, and calculated shear-wave velocity in the upper 30 m (Zalachoris *et al.*, 2017). Published geologic and topographic information of the area inside the buffer zone of potential sites was used to identify firmness of the substrate. Areas of higher elevation and stiffer formations were preferred over sites located in basins and atop recent sediments. Areas with heavy traffic were avoided. Additional considerations for site suitability included verification of mobile data network coverage for fast data upload and remote-equipment communication and drilling-rig accessibility for station installation and routine maintenance. Each potential permanent-station site was screened for excessive ambient noise using a 24 hr test.

One criterion of a successful 24 hr noise test was median noise at least 20 dB below that of the USGS new high-noise model (NHNM) for all frequency bands (Peterson, 1993). For

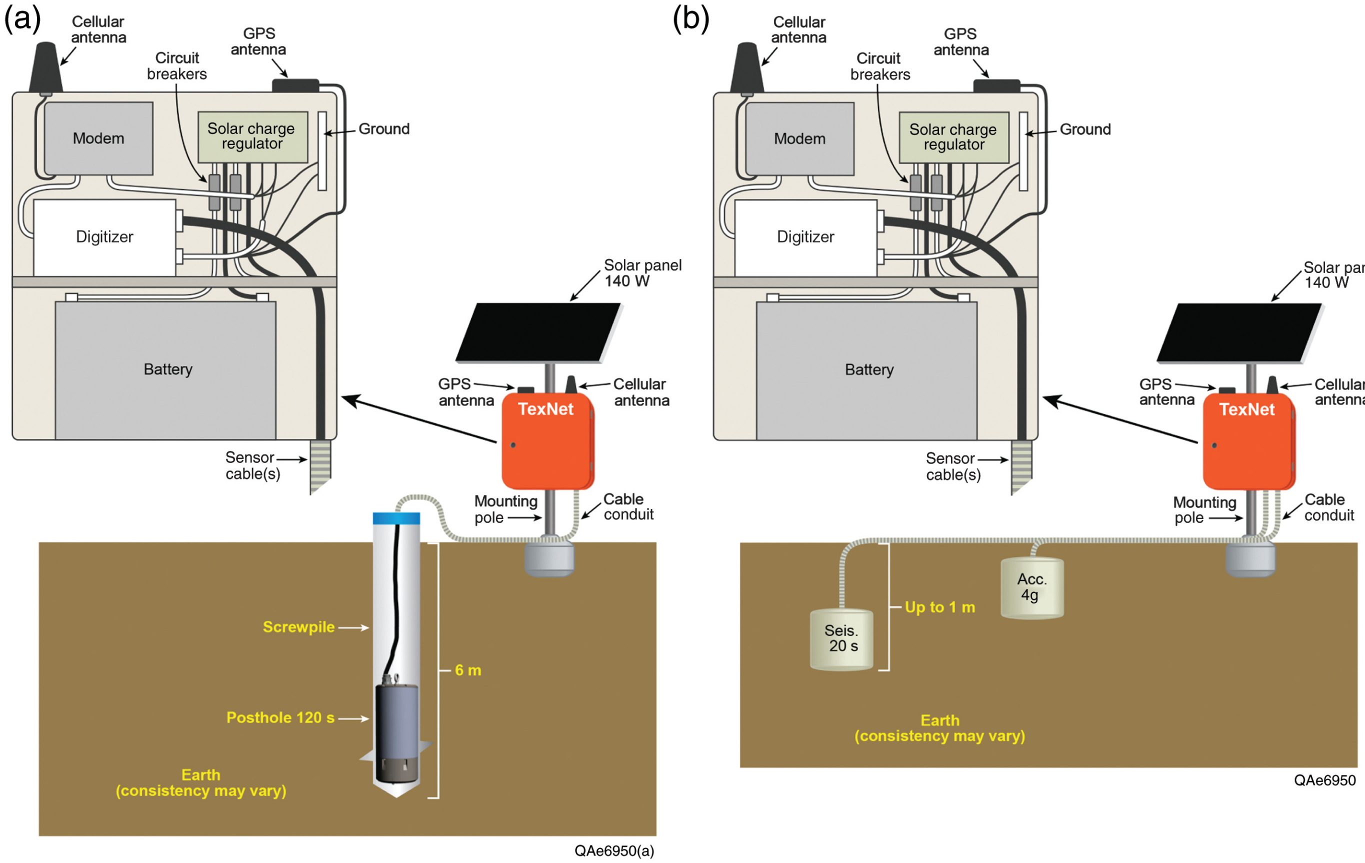

▲ **Figure 3.** Schematic representation of (a) borehole and (b) direct-burial station deployment.

example, noise-test results of all orthogonal components for potential site ET11 show that because the median noise was higher than the specified limit (Ⓔ Fig. S1, available in the supplemental content to this article), the site was rejected from deployment consideration.

Portable Sites. Portable sites (Fig. 3) were selected on the basis of two principal criteria: (1) the ability to reduce uncertainty of hypocentral information for seismically active areas and (2) the capability of fast deployment to new areas of seismic activity, including physical accessibility to the site. Because a portable network covers a smaller area than that of a permanent network, flexibility is limited in repositioning sites away from sources of surface noise.

Site Selection

Permanent Stations. Field locations visited in the process of identifying the best possible sites for installing permanent borehole stations are shown in Ⓔ Table S1. In areas where nearby human activity might produce excessive noise, numerous sites and landowners were identified for consideration, providing more options for final site selection. Up to 21 potential sites were identified in the search for each final site location at each station. We visited 70 out of 167 sites being considered for a 24 hr noise test for permanent borehole-station installation. Of those, 22 sites passed the noise-test criteria and were used for station installation. All stations had been deployed by August 2017.

Portable Stations. Site evaluation of portable stations was similar to that of permanent stations, except that modification of original locations was not possible, and 24 hr noise tests were not often conducted *a priori*. For portable-station locations where we did not conduct a noise test, noise was estimated by visual inspection of the area, and noise level after station deployment was evaluated annually. In the case of high-noise conditions, stations will be moved to a new site.

QA of Stations

State-of-health information for all stations is available to the TexNet team. Up to the present (January 2017–September 2018), the network has been experiencing more than 99% uptime. So that data quality could be evaluated, we applied a noise analysis to the time series of all orthogonal components from January through May 2018 (Ⓔ Fig. S2).

QA assessment (Fig. 4) for stations deployed through end of 2017 shows that, out of the 25 backbone network stations, no stations indicated high noise and only 7 stations indicated noise levels close to the limit threshold (−20 db below NHNM). The latter group can be attributed to increased industrial activity near the stations after initial site assessment.

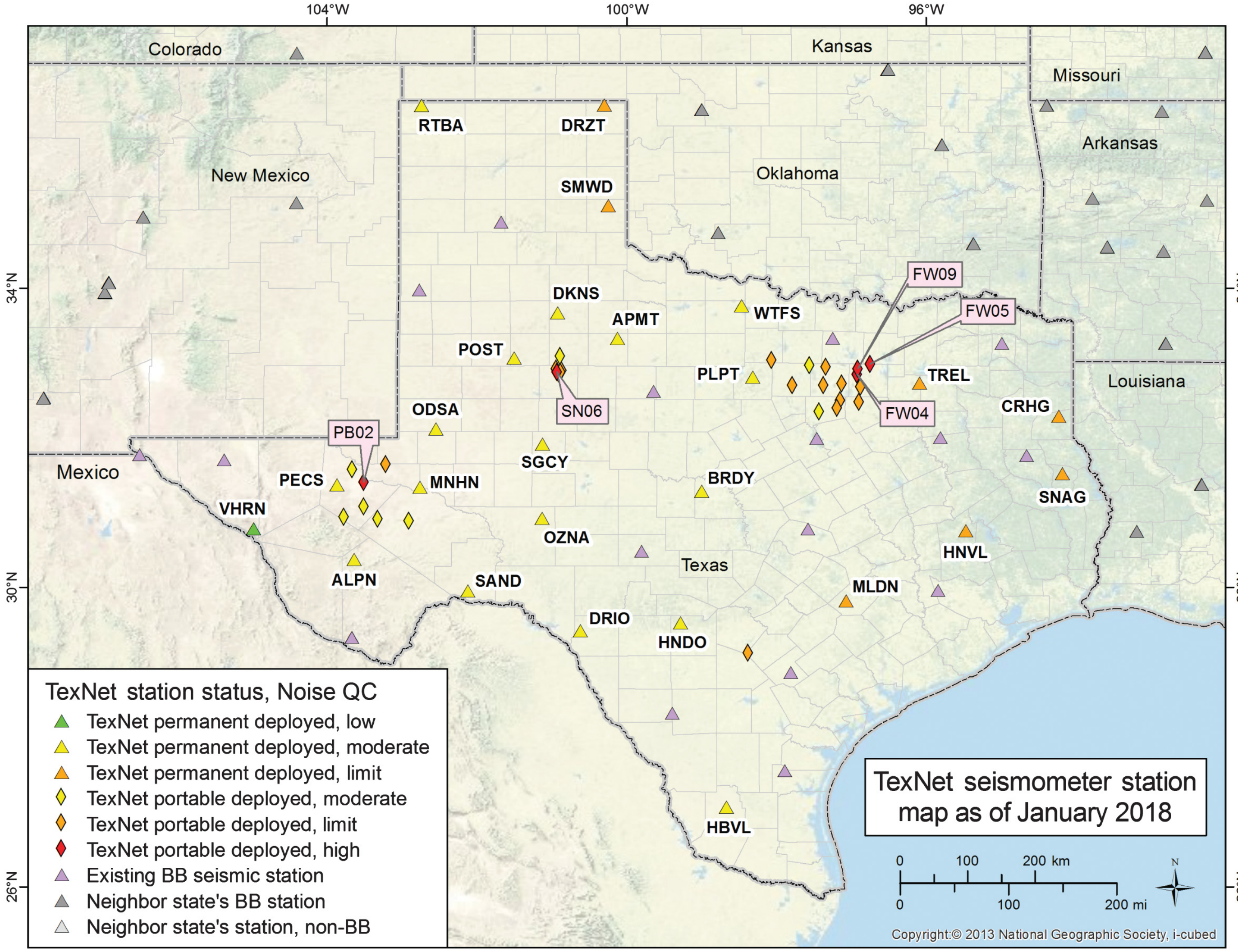

▲ **Figure 4.** Current station map with noise characteristics (low, moderate, limit, high) as of January 2018.

Out of the 29 portable stations deployed by the end of 2017, 5 stations were found to have high noise.

TEXNET DATA AND EARTHQUAKE EVENT MANAGEMENT

TexNet Data Hub

Real-time ground-motion data (raw time series) are recorded from each sensor and archived locally in the TexNet data hub. In case of cell-coverage failure, locally stored time-series data are transmitted when the network connection is re-established. Every night, an automatic workflow checks for data gaps and backfills the archive in the TexNet data hub when possible.

The Data Management Center (Fig. 5) stores data for four months in a real-time ring buffer (server 1), archived locally, and the data are also fed into the EMS for real-time event identification (server 2). The time-series data are stored on server 2 (backup 1) and are also archived in The University of Texas at Austin cloud infrastructure (server 3—backup 2). Through server 3, earthquake data and related information are available to the public through the SeedLink protocol (real time), ArcLink protocol (archive), and International Federation of Digital Seismograph Networks (FDSN) web services. Both Incorporated Research Institutions for Seismology (IRIS; see Data and Resources) and National Earthquake Information Center (NEIC; see Data and Resources) have a direct SeedLink connection to our public SeedLink archive (server 3).

Ground-motion data from existing seismic stations in Texas and neighboring states are acquired from IRIS and used by the EMS. The latter employs an earthquake event identification module that processes in real time any new event. An automatic event location is calculated, an e-mail is sent automatically to the TexNet operations team, and a revised event location is provided after human intervention. Final earthquake-source information is stored in the EMS database and made available to the public through the TexNet earthquake catalog website (see Data and Resources).

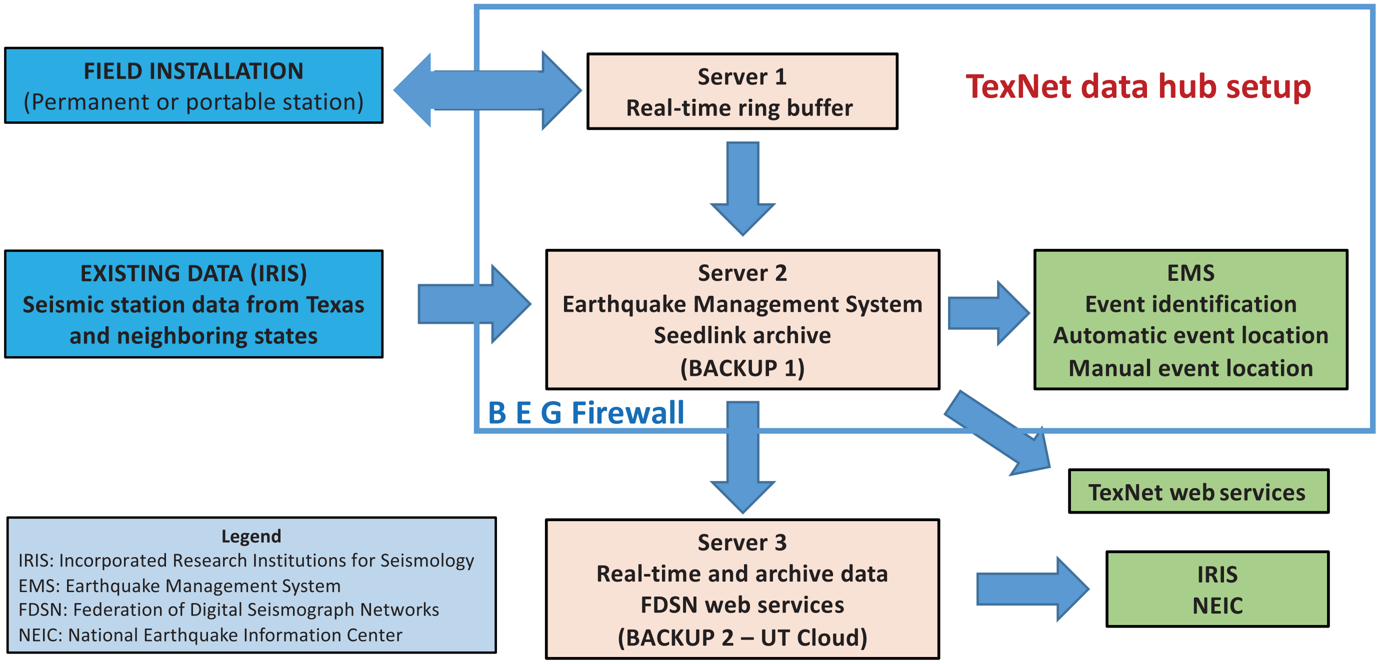

▲ **Figure 5.** Schematic representation of TexNet data hub with data-flow information.

EMS

SeisComP3 (SCP3) software (see Data and Resources) is used for the EMS. SCP3 is seismology software for data acquisition, processing, distribution, and interactive analysis that was developed by the GEOFOrschungsNetz (GEOFON) program (see Data and Resources) at Helmholtz-Zentrum Potsdam, GeoForschungsZentrum (GFZ) German Research Centre for Geosciences (see Data and Resources), and gempa GmbH (see Data and Resources). SCP3 is a fully modular system that is used worldwide (Ⓔ Fig. S3) in systems ranging from offline ground-motion evaluation to early warning systems. Through SCP3, TexNet is able to retrieve data from different vendor data-acquisition servers and IRIS. SCP3 also provides TexNet network data to IRIS and NEIC.

Crustal-Velocity Models

To optimize velocity structure used in the earthquake-location process, TexNet considered previous studies (e.g., Mitchell and Landisman, 1971; Keller and Shurbet, 1975; Orr, 1984; Doser *et al.*, 1992; Kissling *et al.*, 1994; Bilich *et al.*, 1998; Frohlich *et al.*, 2011, 2012, 2014; Hermann *et al.*, 2011; Frohlich, 2012; Frohlich and Brunt, 2013; Gan and Frohlich, 2013; Hornbach *et al.*, 2015; Walter *et al.*, 2016; Borgdfelt, 2017; Nakai *et al.*, 2017; Scales *et al.*, 2017; Quinones *et al.*, 2018) that discuss the velocity structure of Texas, as well as regional seismic profiles. Various independent and combined models are used to identify optimal crustal velocities according to origin-time residuals.

TexNet uses, for areas other than Delaware basin (Fig. 2), the International Association of Seismology and Physics, 1991 (IASP91) Earth model (see Data and Resources) for earthquake location. However, most of the reported seismicity for 2017 (Savvaidis *et al.*, 2017) is located in west Texas (i.e., Delaware basin). To minimize earthquake-location uncertainties specific to the Delaware basin, TexNet uses an optimized 1D (DB1D; Huang *et al.*, 2017) Earth model (Fig. 6a), which emanated from velocity models obtained from previous studies (Orr, 1984; Doser *et al.*, 1992; Borgdfelt, 2017; Nakai *et al.*, 2017) and was optimized using seismic tomography (Roecker *et al.*, 2004, 2006). This process of creating site-specific velocity models has been used by numerous researchers (Doser *et al.*, 1992; Borgdfelt, 2017; Nakai *et al.*, 2017; Scales *et al.*, 2017; Quinones *et al.*, 2018). The Earth models used for earthquake location in the Delaware basin (DB1D) and the rest of the state (IASP91) are presented in Figure 6b. *P*- and *S*-wave velocities for DB1D are provided in Ⓔ Table S2.

Earthquake Detection, Analysis, Quality Control, Cataloging, and Notification

Automated event detection is based on the calculation of signal-to-noise ratio for each seismic station. Short-time average over long-time average calculations are used for automatic phase picks. In addition, we apply an enhanced *S*-picker module, based on an *S*-Akaike information criterion algorithm (Grigoli *et al.*, 2018). Specific band-pass filters that distinguish between local and regional events are applied to the time series. We developed one pipeline (for the whole state) for detecting regional seismicity and four pipelines (one for each area where portable stations are deployed) for detecting local microseismicity. All qualified triggers from each station are next registered in the EMS, which then clusters the triggers to estimate the origin time of a seismic event.

The original location and time for each earthquake event are automatically generated by the SCP3 software. TexNet analysts then verify the location and refine it by applying a global search-location algorithm NonLinLoc (Lomax *et al.*, 2000, 2009). Local magnitude (M_L) information is calculated for the whole state using the formula (equation 2 on supplement S01) of Scales *et al.* (2017) that is based on an attenuation relationship derived from earthquake data in the Dallas–Fort Worth basin. Final location, magnitude, and origin times for each seismic event are based on a minimum travel-time residual between measured arrival times from the seismometers and calculated arrival times. Analysts also remove any false-positive events if they do not fall into any of three categories: earthquakes, quarry blasts, or nonlocatable. Only those events identified as earthquakes are included in the public catalog.

The verified origin time, location, and magnitude of earthquakes are archived and published on the TexNet earthquake information website (see Data and Resources) for public reference.

MAGNITUDE OF COMPLETENESS

In Figure 7a, we present the M_c for the whole state based on observed earthquake data from January 2017 through September 2018. We used the Bayesian magnitude of completeness (BMC) method (Mignan *et al.*, 2011) that requires seismic stations' location information in addition to the earthquake catalog. Based on this result, we plan to increase the number of stations in key areas where seismicity is reported or the interstation distance is high.

FMD from January 2017 through September 2018 for (1) Delaware basin (Fig. 7b) and (2) Snyder (Fig. 7c) is presented. The GFT, MAXC mean, and the median-based analysis of the segment slope methods (Mignan and Woessner, 2012) are used for the M_c calculations in both Delaware basin and Snyder.

DISCUSSION

Earthquakes in Texas over the last decade occurred in areas of high-socioeconomic interest and remain areas of focused study for TexNet portable systems, research, and collaboration. A plethora of peer-reviewed publications based on regional or local seismic networks now exist (Frohlich *et al.*, 2011, 2014, 2016; Frohlich, 2012; Frohlich and Brunt, 2013; Hornbach *et al.*, 2015, 2016; Walter *et al.*, 2016, 2018).

Seismicity has been reported through the TexNet public website from January 2017 through September 2018 (Fig. 8), and the portable networks up to that time are spread out in four different areas that denote higher seismicity. In total, 4638 earthquakes are reported for this period, and of those events, 148 are $2.5 \le M_L \le 3.6$.

However, over the 2017–2018 operations of TexNet, the Delaware basin in west Texas generated the largest number of earthquakes. Therefore, we chose Delaware basin seismicity for exploring network performance to resolve earthquake hypocentral information in areas with joint backbone and portable instrumentation.

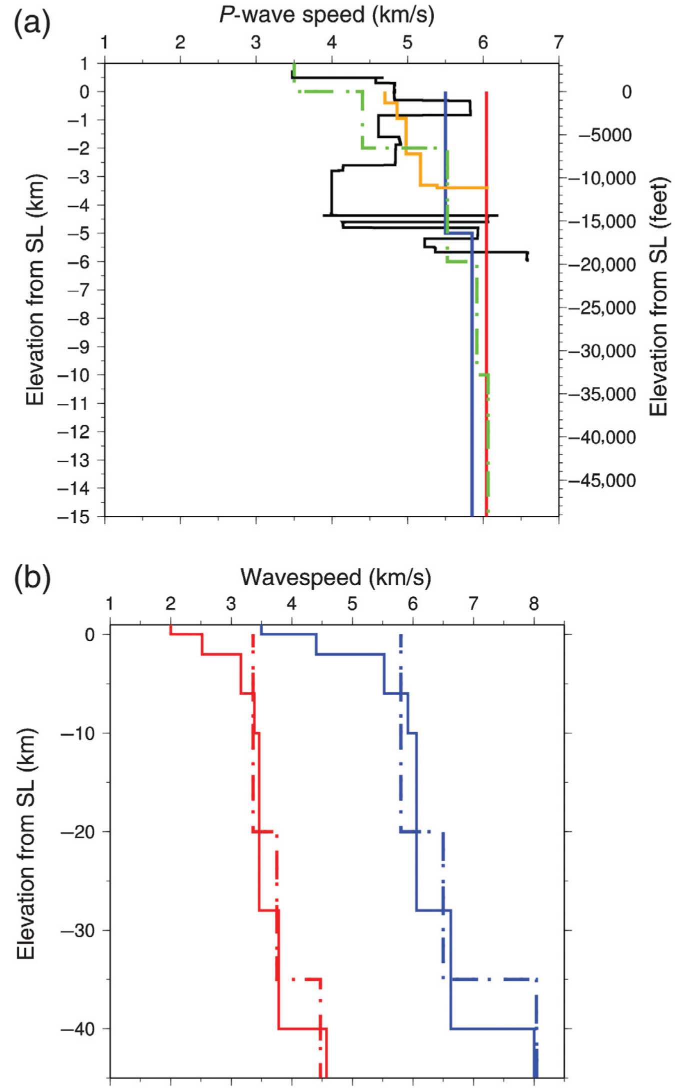

▲ **Figure 6.** (a) 1D Earth model (DB1D) utilized for earthquake locations in the Delaware basin (green dotted–dashed line). Earth models available from the literature also presented in different colors: Orr (1984, orange); Doser *et al.* (1992, black); Borgdfelt (2017, blue); Nakai *et al.* (2017, red). (b) *P*- and *S*-wave 1D Earth models, DB1D (solid line), and International Association of Seismology and Physics, 1991 (IASP91) Earth model (see Data and Resources) (dotted–dashed line) used for earthquake location in the Delaware basin and the rest of the state, respectively.

We relocated the total population of earthquakes (2248 events) provided through the TexNet catalog for the Delaware basin using (1) only existing pre-TexNet stations, (2) existing pre-TexNet stations and TexNet backbone stations, or (3) all stations (Fig. 9). As expected, the number of phases available for earthquake location increases from 5 to 6 using only existing pre-TexNet stations and to more than 18 with all stations being considered. Furthermore, for most of the available events, the body-wave separation azimuthal gap (GAP) decreases from a mean of 200° using pre-TexNet stations, to less than 80° using all stations.

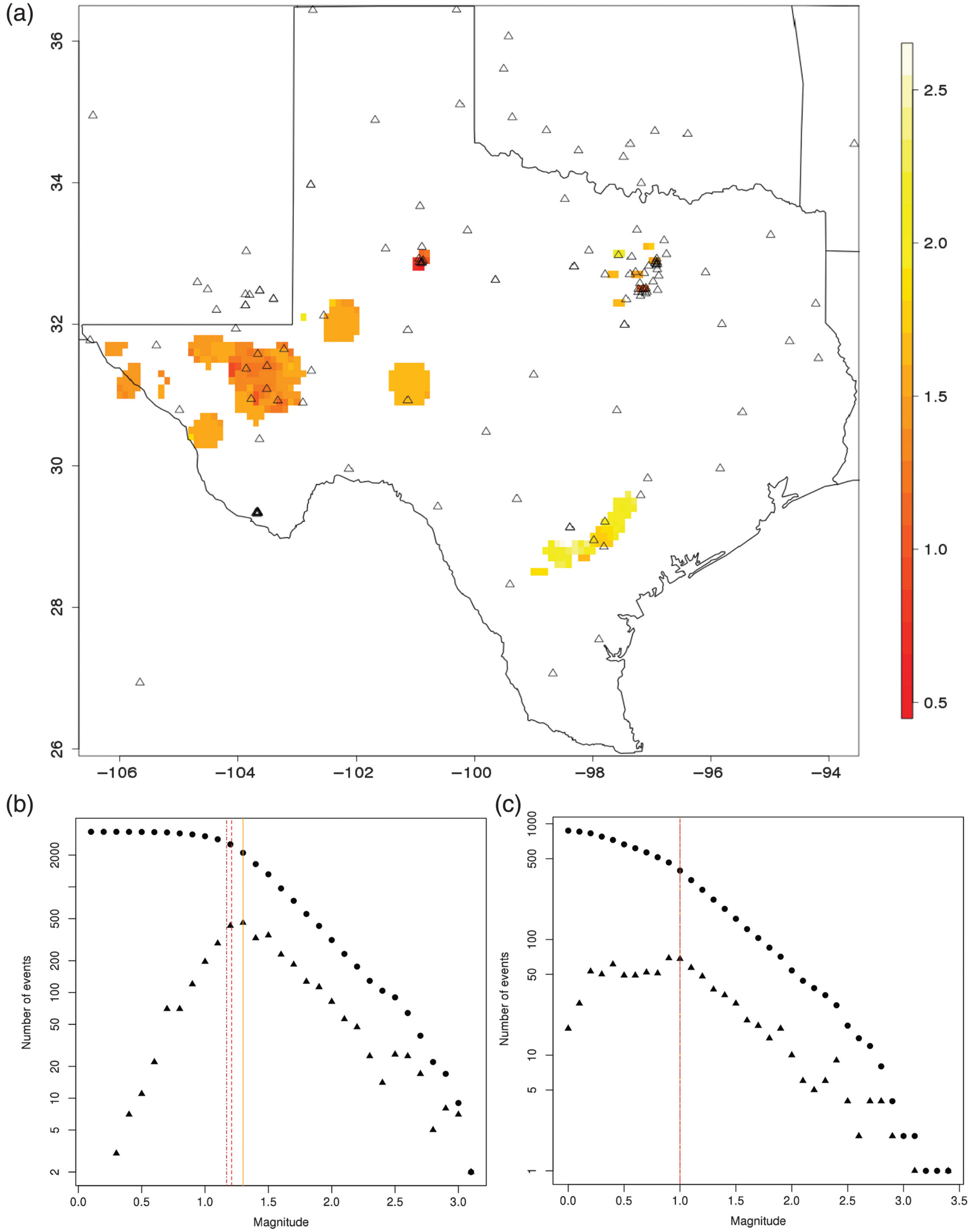

▲ **Figure 7.** Magnitude of completeness (M_c) for TexNet from January 2017 through September 2018 utilizing observed seismicity for (a) whole state based on Bayesian magnitude of completeness (BMC) spatial mapping, (b) Delaware basin, and (c) Snyder. In plots (b) and (c) the goodness of fit (GFT, dotted–dashed line), the maximum curvature (MAXC) mean (dashed line), and median based analyses of the segment slope (solid line) is shown. Specifically, for Snyder (c) all methods provide the same M_c value.

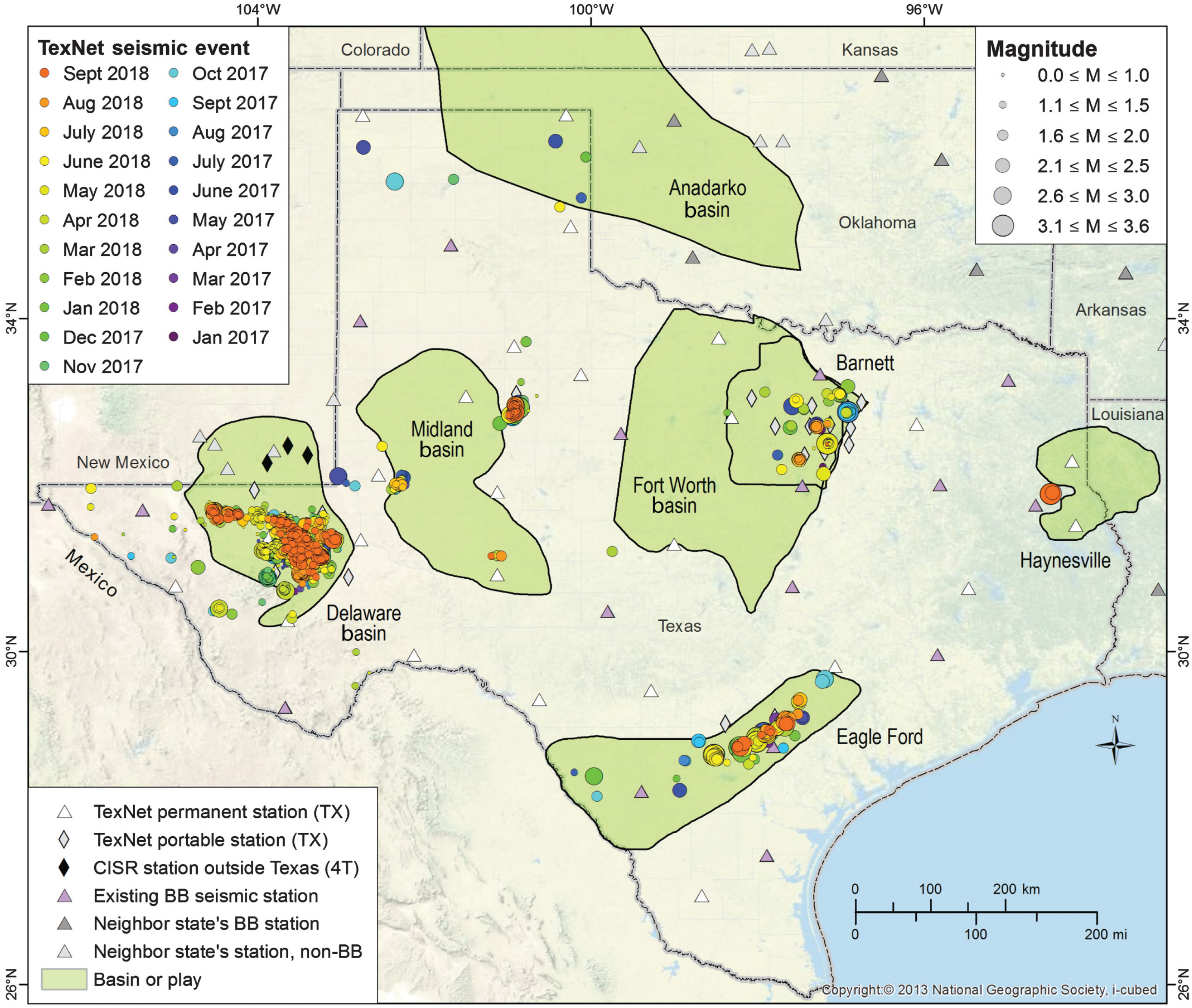

▲ **Figure 8.** Earthquakes publicly reported from TexNet for Texas, from January 2017 through September 2018.

We observed large changes in the horizontal and vertical uncertainties prior to and following TexNet. When we used only existing, pre-TexNet stations, horizontal uncertainties were larger than 5 km, and depth uncertainties were larger than 7 km for most of the Delaware earthquakes. With all stations, horizontal uncertainties reduce to 1.5 km and vertical uncertainties to less than 3 km. Without the new TexNet stations, we were able to provide earthquake-source information for only 1468 events out of 2248. Also in this case, when global search-location techniques were used, epicentral location and hypocentral-depth uncertainties were much higher than they were in calculations that included the TexNet stations. In Figure 10, we present the horizontal distance that epicenters moved when event location is calculated with and without TexNet stations in the Delaware basin.

CONCLUSIONS

During the period of 2016 through 2017, TexNet deployed 58 new broadband seismic stations in Texas. Of these, 25 were added to the existing 18 broadband stations, creating an evenly spaced backbone, seismic network of the state. An additional 33 portable stations were deployed in four different areas of recent seismicity and of high-socioeconomic impact.

An EMS was adopted to detect, analyze, and provide earthquake-source information to the public, and a plan to analyze the earthquakes using $M_L \geq 2$ by the next business day was put into effect. Smaller earthquakes are available on our earthquake catalog website that prioritizes higher magnitudes, and TexNet provides the information necessary to support earthquake-related research in Texas. By decreasing M_c and the

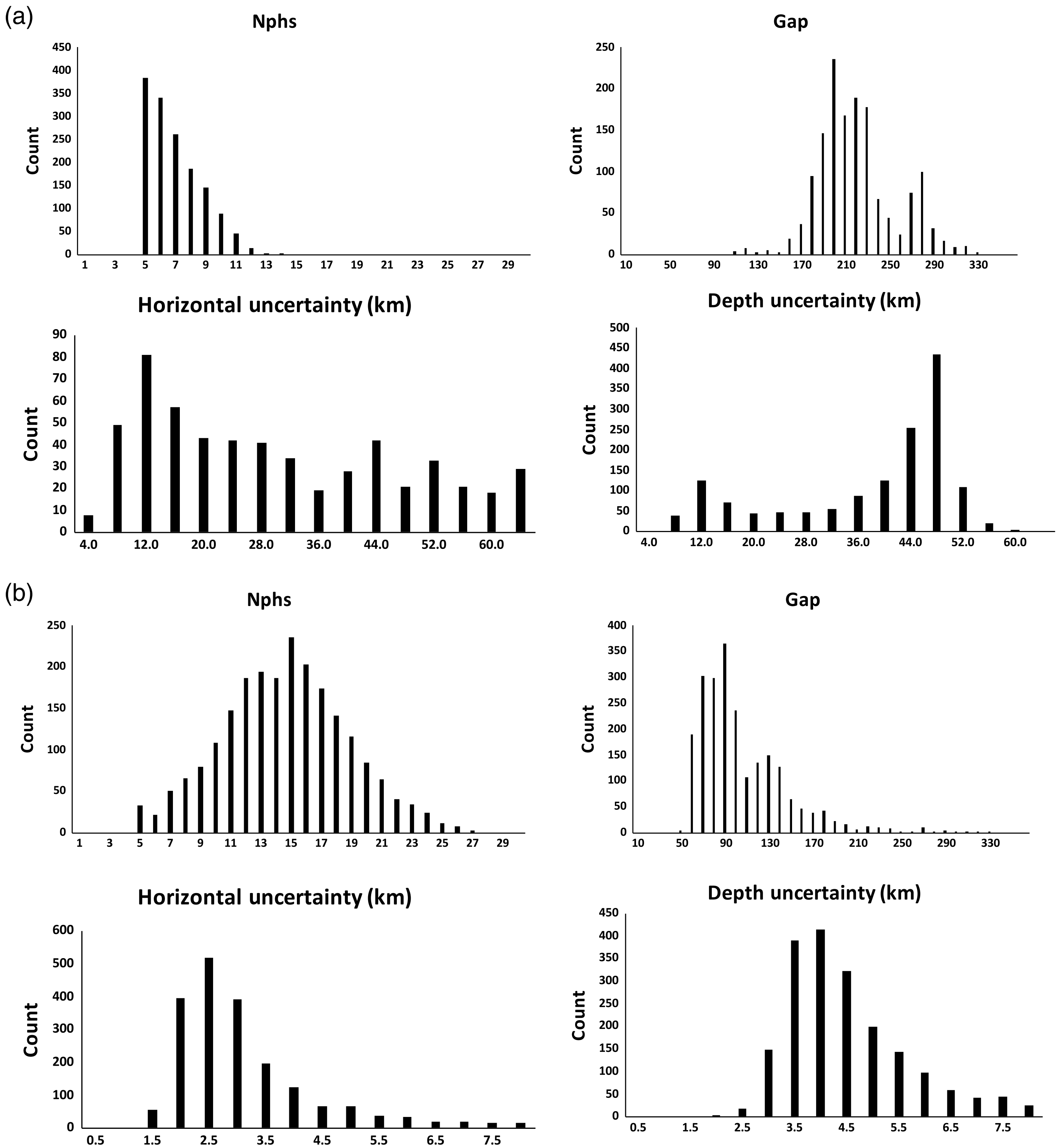

▲ **Figure 9.** Comparison of event-location statistical parameters in the Delaware basin with (a) only existing pre-TexNet stations (only distribution of uncertainties of up to 8 km presented), (b) existing and TexNet backbone stations, and (c) existing, TexNet backbone, and portable stations. (*Continued*)

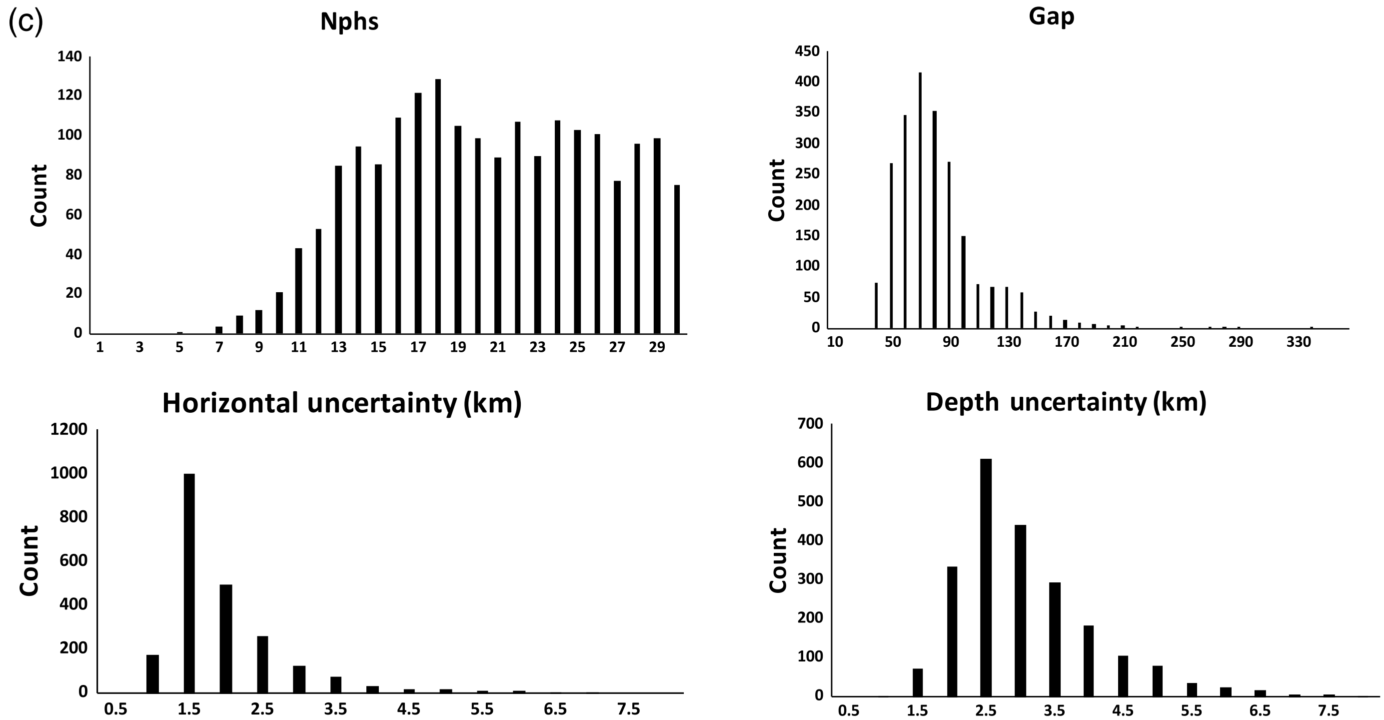

Figure 9. Continued.

uncertainty in an earthquake location, TexNet is expected to boost scientific advancements in explaining causation of reported seismicity in the state.

DATA AND RESOURCES

Texas Seismological Network (TexNet) has currently three network codes on the International Federation of Digital Seismograph Networks: TX is for the backbone and portable stations (https://doi.org/10.7914/SN/TX), 4T is for stations deployed in neighboring states to better locate earthquakes in Texas (https://doi.org/10.7914/SN/4T_2018), and 2T is for temporary deployments (https://doi.org/10.7914/SN/2T_2018). Waveform data and metadata information for all stations are available through Incorporated Research Institutions for Seismology (IRIS) and TexNet Federation of Digital Seismograph Networks Web Services (FDSNWS, http://rtserve.beg.utexas.edu/fdsnws/). TexNet catalog information is available through our public website available at http://www.beg.utexas.edu/texnet/catalog/. Metadata and seismograms used in this study were collected except from TexNet stations (network codes TX and 4T) from other networks in the state and neighboring states with the following Federated Digital Seismic Network codes: IM (International Miscellaneous Stations, available at https://www.fdsn.org/networks/detail/IM/), IU (Global Seismographic Network, available at https://doi.org/10.7914/SN/IU), N4 (U.S. Geological Survey [USGS], available at https://doi.org/10.7914/SN/NQ), MX (Mexican National Seismic Network, available at https://doi.org/10.21766/SSNMX/SN/MX), OK (Oklahoma Geological Survey, available at https://doi.org/10.7914/SN/OK), SC (New Mexico Tech Seismic Network, available at https://www.fdsn.org/networks/detail/SC/), TA (USArray Transportable Array, available at https://doi.org/10.7914/SN/TA), US (United States National Seismic Network, available at https://doi.org/10.7914/SN/US), ZP (Seismic Investigation of South Central Oklahoma, available at https://doi.org/10.7914/SN/ZP_2016), ZW (Southern Methodist University [SMU], available at https://doi.org/10.7914/SN/ZW_2013), and 4F (SMU, available at https://doi.org/10.7914/SN/4F_2015). The IRIS Mustang webservices and the USGS Comprehensive Catalog (ComCat) were used for this study. USGS/Advanced National Seismic System (ANSS) ComCat is

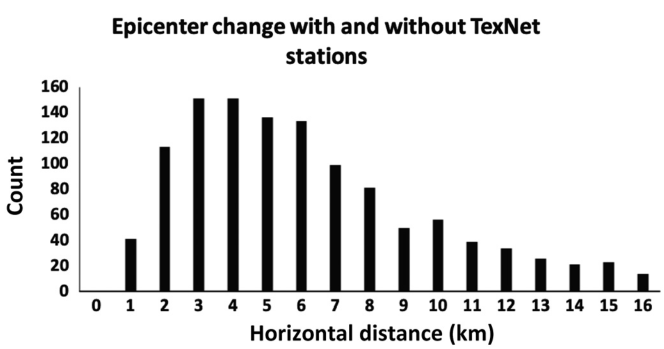

▲ **Figure 10.** Change of epicenter (horizontal distance in km) between earthquake locations calculated with and without TexNet stations.

available at https://earthquake.usgs.gov/data/comcat/. IRIS website can be accessed at http://www.iris.edu. National Earthquake Information Center (NEIC) can be accessed at https://earthquake.usgs.gov/contactus/golden/neic.php. SeisComP3 (SCP3) software is available at http://www.seiscomp3.org/. GEOFON program is available at http://geofon.gfz-potsdam.de/. GeoForschungsZentrum (GFZ) German Research Centre for Geosciences is available at http://www.gfz-potsdam.de/. Gempa GmbH is available at http://www.gempa.de/. The International Association of Seismology and Physics, 1991 (IASP91) Earth model is available at https://ds.iris.edu/ds/products/emc-iasp91. All websites were last accessed on December 2018.

ACKNOWLEDGMENTS

The authors would like to thank the State of Texas for funding the Texas Seismological Network (TexNet) and the TexNet Advisory Committee for providing valuable feedback throughout deployment of the network. The authors would like to thank the personnel of the Bureau of Economic Geology at The University of Texas at Austin and Southern Methodist University, both of whom participated in site assessment and the deployment of stations. Special thanks to two anonymous reviewers and the associate editor for their productive comments. Publication authorized by the Director, Bureau of Economic Geology.

REFERENCES

Bilich, A., S. A. Clark, B. Creighton, and C. Frohlich (1998). Felt reports from the Alice, Texas, earthquake of 24 March 1997, *Seismol. Res. Lett.* **69,** 117–122.

Borgdfelt, T. (2017). Crustal seismic velocity models of Texas, *Master's Thesis*, The University of Texas at Austin, 86 pp.

Casey, R., M. Templeton, G. Sharer, L. Keyson, B. Weertman, and T. Ahern (2018). Assuring the quality of IRIS data with MUSTANG, *Seismol. Res. Lett.* **89,** no. 2A, 630–639, doi: 10.1785/0220170191.

Doser, D., M. R. Baker, M. Luo, P. Marroquin, L. Balesteros, J. Kingwell, H. Diaz, and G. Kaip (1992). The not so simple relationship between seismicity and oil production in the Permian Basin, West Texas, *Pure Appl. Geophys.* **139,** 481–506.

Ellsworth, W. L. (2013). Injection-induced earthquakes, *Science* **341,** 1225942, 7, doi: 10.1126/science.1225942.

Frohlich, C. (2012). Two-year survey comparing earthquake activity and injection well locations in the Barnett Shale, Texas, *Proc. Natl. Acad. Sci.* **109,** 13,934–13,938, doi: 10.1073/pnas.1207728109.

Frohlich, C., and M. Brunt (2013). Two-year survey of earthquakes and injection/production wells in the Eagle Ford Shale, Texas, prior to the M_W4.8 20 October 2011 earthquake, *Earth Planet. Sci. Lett.* **379,** 53–63, doi: 10.1016/j.epsl.2013.07.025.

Frohlich, C., and S. Davis (2002). *Texas Earthquakes*, University of Texas Press, Austin, Texas, 275 pp.

Frohlich, C., H. R. DeShon, B. W. Stump, C. Hayward, M. J. Hornbach, and J. I. Walter (2016). A historical review of induced earthquakes in Texas, *Seismol. Res. Lett.* **87,** 1022–1038, doi: 10.1785/0220160016.

Frohlich, C., W. L. Ellsworth, W. A. Brown, M. Brunt, J. H. Luetgert, T. MacDonald, and S. Walter (2014). The 17 May 2012 M4.8 earthquake near Timpson, east Texas: An event possibly triggered by fluid injection, *J. Geophys. Res.* **119,** 581–593, doi: 10.1002/2013JB010755.

Frohlich, C., J. Glidewell, and M. Brunt (2012). Location and felt reports for the 25 April 2010 mbLg3.9 earthquake near Alice, Texas: Was it induced by petroleum production? *Bull. Seismol. Soc. Am.* **102,** 457–466, doi: 10.1785/0120110179.

Frohlich, C., C. Hayward, B. W. Stump, and E. Potter (2011). The Dallas-Fort Worth earthquake sequence: October 2008 through May 2009, *Bull. Seismol. Soc. Am.* **101,** 327–340, doi: 10.1785/0120100131.

Gan, W., and C. Frohlich (2013). Gas injection may have triggered earthquakes in the Cogdell oil field, Texas, *Proc. Natl. Acad. Sci. Unit. States Am.* **110,** 18,786–18,791, doi: 10.1073/pnas.1311316110.

Grigoli, F., L. Scarabello, M. Boese, B. Weber, S. Wiemer, and J. F. Clinton (2018). Pick- and waveform-based techniques for real-time detection of induced seismicity, *Geophys. J. Int.* **213,** no. 2, doi: 10.1093/gji/ggy019.

Hermann, R. B, H. Benz, and C. J. Ammon (2011). Monitoring the earthquake source process in North America, *Bull. Seismol. Soc. Am.* **101,** 2609–2625.

Hornbach, M. J., H. R. DeShon, W. Ellsworth, B. Stump, C. Hayward, C. Frohlich, H. Oldham, J. Olson, M. Magnani, C. Brokaw, and J. Luetgert (2015). Causal factors for seismicity near Azle, Texas, *Nat. Comm.* **6,** 1–11, doi: 10.1038/ncomms7728.

Hornbach, M. J., M. Jones, M. Scales, H. R. DeShon, M. B. Magnani, C. Frohlich, B. W. Stump, C. Hayward, and M. Layton (2016). Ellenburger wastewater injection and seismicity in North Texas, *Phys. Earth Planet. In.* **261,** Part A, 54–68, doi: 10.1016/j.pepi.2016.06.012.

Huang, G.-C. D., C. Aiken, A. Savvaidis, B. Young, and J. Walter. (2017). Improving the velocity structure in the Delaware basin of West Texas for seismicity monitoring, *Eos Trans. AGU* S23C–0836.

Keller, G. R., and D. H. Shurbet (1975). Crustal structure of the Texas Gulf Coastal plain, *GSA Bull.* **86,** 807–810.

Kissling, E., W. L. Ellsworth, D. Eberhart-Phillips, and U. Kradolfer (1994). Initial reference models in local earthquake tomography, *J. Geophys. Res.* **99,** 19,635–19,646.

Lomax, A., A. Michelini, and A. Curtis (2009). Earthquake location, direct, global-search methods, in *Encyclopedia of Complexity and System Science*, Part 5, C. H. Thurber and N. Rabinowitz (Editors), Springer, New York, New York, 2449–2473, doi: 10.1007/978-0-387-30440-3.

Lomax, A., J. Virieux, P. Volant, and B. C. Thierry (2000). Probabilistic earthquake location in 3D and layered models: Introduction of a Metropolis–Gibbs method and comparison with linear locations, in *Advances in Seismic Event Location*, C. H. Thurber and N. Rabinowitz (Editors), Kluwer Academic, Dordrecht, The Netherlands, 101–134.

McNamara, D. E., C. R. Hutt, L. S. Gee, H. M. Benz, and R. P. Buland (2009) A method to establish seismic noise baselines for automated station assessment, *Seismol. Res. Lett.* **80,** 628–637.

Mignan, A., and J. Woessner (2012). Estimating the magnitude of completeness for earthquake catalogs, *Community Online Resource for Statistical Seismicity Analysis*, doi: 10.5078/corssa-00180805.

Mignan, A., M. J. Werner, S. Wiemer, C.-C. Chen, and Y.-M. Wu (2011). Bayesian estimation of the spatially varying completeness magnitude of earthquake catalogs, *Bull. Seismol. Soc. Am.* **101,** doi: 10.1785/0120100223.

Mitchell, B. J., and M. Landisman (1971). Geophysical measurements in the southern great plains, in *The Structure and Physical Properties of the Earth's Crust*, J. G. Heacock (Editor), American Geophysical Monograph 24, 77–92.

Nakai, J. S., A. F. Sheehan, and S. L. Bilek (2017). Seismicity of the rocky mountains and Rio Grande rift from the EarthScope Transportable Array and CREST temporary seismic networks, 2008–2010, *J. Geophys. Res.* **122,** 2173–2192, doi: 10.1002/2016JB013389.

Orr, C. D. (1984). A seismotectonic study and stress analysis of the Kermit seismic zone, *Ph.D. Dissertation*, The University of Texas at El Paso, 289 pp.

Peterson, J. (1993). Observation and modeling of seismic background noise, *U.S. Geol. Surv. Open-File Rept. 93-322*, 94 pp.

Quinones, L. A., H. R. DeShon, M. B. Magnani, and C. Frohlich (2018). Stress orientations in the Fort Worth Basin, Texas, determined from earthquake focal mechanisms, *Bull. Seismol. Soc. Am.* **108,** no. 3A, 1124–1132, doi: 10.1785/0120170337.

Roecker, S. W., C. Thurber, and D. McPhee (2004). Joint inversion of gravity and arrival time data from Parkfield: New constraints on structure and hypocenter locations near SAFOD drill site, *Geophys. Res. Lett.* **31,** doi: 10.1029/2003GL019396.

Roecker, S. W., C. Thurber, K. Roberts, and L. Powell (2006). Refining the image of the San Andreas Fault near Parkfield, California, using a finite difference travel time computation technique, *Tectonophysics* **426,** 189–205.

Savvaidis, A., P. Hennings, D. Huang, C. Aiken, B. Young, and J. Osmond (2017). A first look at active seismicity in the Delaware Basin (West Texas), *SEG/SPE Workshop on Injection Induced Seismicity*, 6–8 November, Dallas, Texas.

Scales, M. M., H. R. DeShon, M. B. Magnani, J. I. Walter, L. Quinones, T. L. Pratt, and M. J. Hornbach (2017). A decade of induced slip on the causative fault of the 2015 Mw 4.0 Venus earthquake, northeast Johnson County, Texas, *J. Geophys. Res.* **122,** 7879–7894, doi: 10.1002/2017JB014460.

Walter, J. I., P. J. Dotray, C. Frohlich, and J. F. W. Gale (2016). Earthquakes in northwest Louisiana and the Texas–Louisiana border possibly induced by energy resource activities within the Haynesville shale play, *Seismol. Res. Lett.* **87,** 285–294, doi: 10.1785/0220150193.

Walter, J., C. Frohlich, and T. Borgfeldt (2018). Natural and induced seismicity in the Texas and Oklahoma Panhandles, *Seismol. Res. Lett.* **89,** no. 6, 2437–2446, doi: 10.1785/0220180105.

Weingarten, M., S. Ge, J. W. Godt, B. A. Bekins, and J. L. Rubinstein (2015). High-rate injection is associated with the increase in U.S. mid-continent seismicity, *Science* **348,** 1336–1340.

Wiemer, S., and M. Wyss (2000). Minimum magnitude of complete reporting in earthquake catalogs: Examples from Alaska, the western United States, and Japan, *Bull. Seismol. Soc. Am.* **90,** 859–869, doi: 10.1785/0119990114.

Wyss, M., A. Hasegawa, S. Wiemer, and N. Umino (1999). Quantitative mapping of precursory seismic quiescence before the 1989, M7.1 off-sanriku earthquake, Japan, *Ann. Geofisc.* **42,** 851–869.

Zalachoris, G., E. Rathje, and P. Jeffrey (2017). V_{S30} characterization of Texas, Oklahoma, and Kansas using the P-wave seismogram method, *Earthq. Spectra* **33,** 943–961.

Alexandros Savvaidis
Bissett Young
Guo-chin Dino Huang
Bureau of Economic Geology
The University of Texas at Austin
University Station, Box X
Austin, Texas 78713-8924 U.S.A.
alexandros.savvaidis@beg.utexas.edu
bissett.young@beg.utexas.edu
dino.huang@beg.utexas.edu

Anthony Lomax
ALomax Scientific
320 Chemin des Indes
06370 Mouans-Sartoux, France
anthony@alomax.net

Published Online 5 June 2019